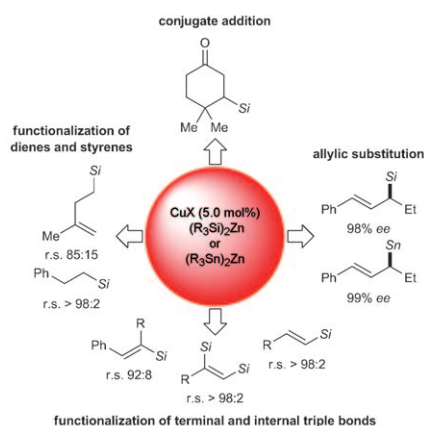


**Go catalytic!** Simple transmetalation from lithium to zinc attenuates the basicity and nucleophilicity of silicon and tin main group organometallics, thereby rendering the stoichiometric use of copper superfluous. All common carbon–silicon and selected carbon–tin bond formations are now catalytic in copper (see scheme; r.s. = regioselectivity).



### Main Group Chemistry

A. Weickgenannt,  
M. Oestreich\* ..... 402–412

### Silicon- and Tin-Based Cuprates: Now Catalytic in Copper!

## COMMUNICATIONS



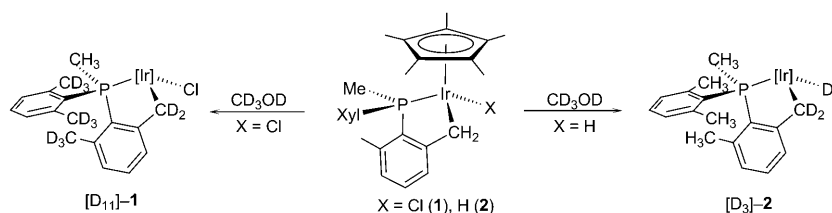
**Chiral is better!** Superior recognition properties are shown by a pyrrolic tripodal receptor featuring a chiral diamine in its architecture. Highly enantioselective recognition of the

$\beta$ -mannosyl residue is achieved by one of the two enantiomers of the receptor, with remarkable affinity in a polar medium and distinct  $\alpha/\beta$  selectivity.

### Carbohydrate Recognition

A. Ardá, C. Venturi, C. Nativi,  
O. Francesconi, G. Gabrielli,  
F. J. Cañada, J. Jiménez-Barbero,\*  
S. Roelens\* ..... 414–418

### A Chiral Pyrrolic Tripodal Receptor Enantioselectively Recognizes $\beta$ -Mannose and $\beta$ -Mannosides



**Which way to go?** The cyclometallated compounds  $[(\eta^5\text{-C}_5\text{Me}_5)\text{Ir}(\text{X})\{\text{PMe}(2,6\text{-CH}_2(\text{Me})\text{C}_6\text{H}_3)(2,6\text{-Me}_2\text{C}_6\text{H}_3)\}]$  ( $\text{X} = \text{Cl}, \text{H}, \text{Me}$ ) have been synthesized in high yields and their potential for C–H activation demonstrated. Deute-

rium incorporation into the metallated ligand backbone has been achieved for  $\text{X} = \text{Cl}$  and  $\text{X} = \text{H}$ , with dissimilar results and hence through different reaction pathways.

### C–H Activation


J. Campos, A. C. Esqueda,  
E. Carmona\* ..... 419–422

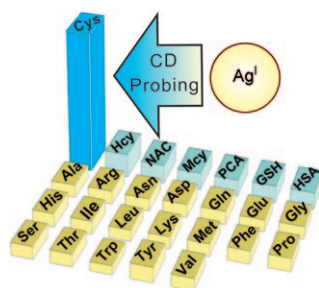
### Cyclometallation and Hydrogen/ Deuterium Exchange Reactions of an Arylphosphine Ligand upon Coordination to $\{\text{Ir}(\eta^5\text{-C}_5\text{Me}_5)\}$



## Cysteine Probe

J. Nan, X.-P. Yan\* ..... 423–427


 **A Circular Dichroism Probe for L-Cysteine Based on the Self-Assembly of Chiral Complex Nanoparticles**



**Silver-assisted detection:** A novel circular dichroism (CD) method was described for detecting L-cysteine in biological fluids on the basis of chiral nanoparticle self-assembly from Ag<sup>+</sup> and L-cysteine (see graphic). The method allows highly selective and sensitive detection of L-cysteine in biological fluids at the  $\mu\text{M}$  level without the need for any special synthesis or sample pretreatment other than an appropriate dilution.

## Nitrogen Heterocycles

D. Tejedor,\* G. Méndez-Abt,  
F. García-Tellado\* ..... 428–431

 **A Convenient Domino Access to Substituted Alkyl 1,2-Dihydropyridine-3-carboxylates from Propargyl Enol Ethers and Primary Amines**



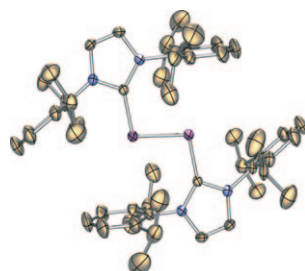
**All at once:** Microwave irradiation of a metal-free mixture of propargyl enol ethers and primary amines generates substituted alkyl 1,2-dihydropyridine-3-carboxylates in excellent yields through a domino process (see

scheme). The obtained 1,2-dihydropyridines feature four possible diversity points and a chemical handle for complexity-diversity generation (carboxylic ester at the C<sub>3</sub> position).

## Diarsenic Compounds

M. Y. Abraham, Y. Wang, Y. Xie,  
P. Wei, H. F. Schaefer, III,  
P. von R. Schleyer,\*  
G. H. Robinson\* ..... 432–435


 **Carbene Stabilization of Diarsenic: From Hypervalency to Allotropy**

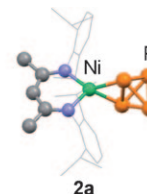
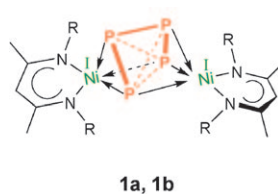


**Diarsenic as a Lewis acid:** An N-heterocyclic carbene stabilized diarsenic molecule [L:As-As:L] (L =  $\text{C}\{\text{N}(2,6\text{-}i\text{Pr}_2\text{C}_6\text{H}_3\text{CH})_2\}$ ) (see scheme) has been prepared by potassium/graphite reduction of [L:AsCl<sub>3</sub>]. The nature of the bonding in this molecule was probed by DFT computations.

## Main Group Chemistry

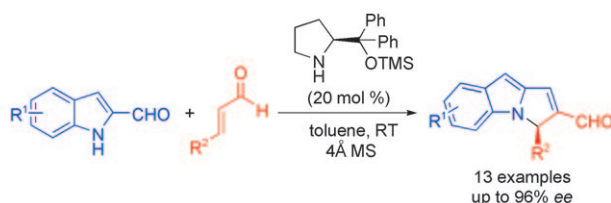
S. Yao, Y. Xiong, C. Milschmann, E. Bill,  
S. Pfirrmann, C. Limberg,  
M. Driess\* ..... 436–439

 **Reversible P<sub>4</sub> Activation with Nickel(I) and an  $\eta^3$ -Coordinated Tetraphosphorus Ligand between Two Ni<sup>I</sup> Centers**



**P<sub>4</sub> activation but without reduction** is the most striking result of the reaction of Ni<sup>I</sup> precursors (LNi) with white phosphorus. This reaction leads to the complexes **1a** and **1b**, which feature the scarce  $\eta^3$ -coordination of the P<sub>4</sub>

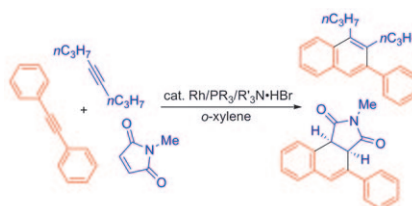
ligand between two metal centers. Remarkably, **1a** undergoes facile dissociation in solution to give the paramagnetic Ni<sup>I</sup> complex **2**. L =  $\beta$ -diketiminate; **1a**: R =  $i\text{Pr}_2\text{C}_6\text{H}_3$ , **1b**: R = 2,6-Et<sub>2</sub>C<sub>6</sub>H<sub>3</sub>.



**Like water from a duck's back:** A highly enantioselective organocatalytic cascade aza-Michael/aldol reaction of indole-2-carbaldehydes with  $\alpha,\beta$ -unsaturated aldehydes has been developed,

providing an easy access to pyrrolo[1,2-*a*]indole-2-carbaldehydes with moderate to excellent enantioselectivities in one single reaction (see scheme).

**Trinity:** The combination of rhodium/phosphine/amine-HBr enables the highly selective catalytic cross-cyclodimerization of diarylacetylenes with aliphatic alkynes to afford the corresponding multiply substituted naphthalenes in good-to-high yields. The catalyst system also allows the use of some alkenes as the coupling partners, which provides a facile route to highly functionalized dihydronaphthalenes (see scheme).



## Asymmetric Catalysis

L. Hong, W. Sun, C. Liu, L. Wang, R. Wang\* ..... 440–444

**Asymmetric Organocatalytic N-Alkylation of Indole-2-carbaldehydes with  $\alpha,\beta$ -Unsaturated Aldehydes: One-Pot Synthesis of Chiral Pyrrolo[1,2-*a*]indole-2-carbaldehydes**



## Cross-Cyclodimerization

K. Sakabe, H. Tsurugi, K. Hirano, T. Satoh, M. Miura\* ..... 445–449

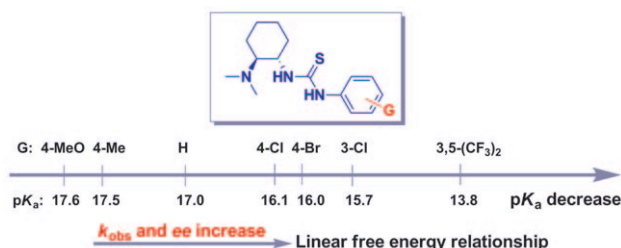
**Rhodium/Phosphine/Amine-HBr Catalyst System for Highly Selective Cross-Cyclodimerization of Aryl- and Alkylalkynes: Efficient Access to Multisubstituted Naphthalene Derivatives**



## Organocatalysis

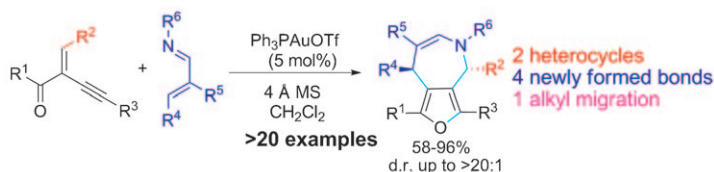
X. Li, H. Deng, B. Zhang, J. Li, L. Zhang, S. Luo,\* J.-P. Cheng\* ..... 450–455

**Physical Organic Study of Structure–Activity–Enantioselectivity Relationships in Asymmetric Bifunctional Thiourea Catalysis: Hints for the Design of New Organocatalysts**



**Acidity effect:** Correlations of pK<sub>a</sub> with catalytic activity and stereoselectivity were determined and linear free energy relationships (LFERs) were observed for both pK<sub>a</sub>–log(*k*) and pK<sub>a</sub>–log(*R/S*) correlations in *meta*-

and/or *para*-substituted aromatic thioureas (see figure). These results provided a basis for new catalyst development and several improved catalysts were identified in our initial attempts.



**Rapid access to heterobicycles:** A novel cationic gold(I)-catalyzed tandem heterobicyclization and 1,2-alkyl migration was developed, which provides a rapid, efficient, and stereoselective access to highly substituted furo[3,4-*c*]azepines from simple, read-

ily available 2-(1-alkynyl)-2-alken-1-ones and  $\alpha,\beta$ -unsaturated imines under mild conditions (see scheme). In contrast, when heteroaryl imines were used, only direct formal [4+3] cycloadducts were formed.

## Domino Reactions

H. Gao, X. Zhao, Y. Yu, J. Zhang\* ..... 456–459

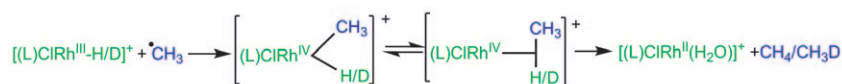
**Highly Substituted Furo[3,4-*c*]azepines by Gold(I)-Catalyzed Diastereoselective Tandem Double Heterocyclizations and 1,2-Alkyl Migration**



## Radical Reactions

L. Kats, E. Maimon,  
D. Meyerstein\* ..... 460–463

### Substantial Inverse Isotope Effects in the Hydrogen Atom Abstraction from $[(L)ClRh^{III}-H/D]^+$ Macrocyclic Complexes by Methyl Radicals in Aqueous Solutions



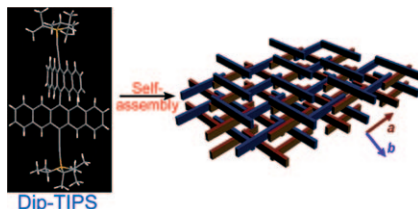
**Inverse gear!** The hydrogen atom abstraction from  $[(L)ClRh^{III}-H/D]^+$  by methyl radicals (see scheme) involves a substantial inverse isotope effect. This result suggests that the

detailed mechanism of this process involves the formation of a transient complex with a Rh–C  $\sigma$  bond followed by reductive elimination.

## Field-Effect Transistors

X. Zhang, X. Jiang, J. Luo, C. Chi,  
H. Chen,\* J. Wu\* ..... 464–468

### A Cruciform 6,6'-Dipentacenyl: Synthesis, Solid-State Packing and Applications in Thin-Film Transistors



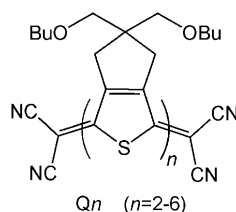
**Get cross!** A cruciform 6,6'-dipentacenyl, Dip-TIPS, was prepared as a unique semiconductor with two-dimensional isotropic face-to-face  $\pi$ -stacking in the crystal structure. High FET mobilities were obtained from the vapor-deposited thin films. The use of cruciform molecules in the design of organic semiconductors is a new concept that is expected to diminish the effect of molecular orientation on device performance.

# FULL PAPERS

## Oligothiophenes

R. Ponce Ortiz, J. Casado,  
S. Rodríguez González, V. Hernández,  
J. T. López Navarrete,\* P. M. Viruela,  
E. Ortí,\* K. Takimiya,  
T. Otsubo ..... 470–484

### Quinoidal Oligothiophenes: Towards Biradical Ground-State Species

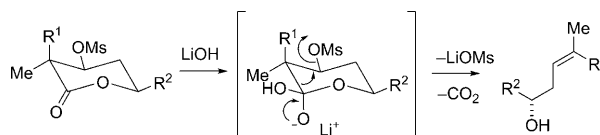


**Ground-state character** of a series of quinoidal oligothiophenes Q2–Q6 ( $n=2-6$  in the depicted formula) was investigated experimentally and by DFT calculations. For Q4–Q6, the latter indicate biradical character that increases with increasing oligomer length. Furthermore, a low-lying triplet state very close in energy to the singlet ground state is predicted. Raman and IR spectra support the quinoidal structures computed for Q2 and Q3 and aromatic biradical structures predicted for Q5 and Q6.

## Natural Products

K. Prantz, J. Mulzer\* ..... 485–506

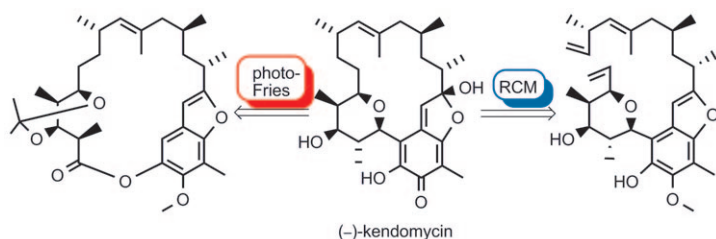
### Synthesis of (Z)-Trisubstituted Olefins by Decarboxylative Grob-Type Fragmentations: Epothilone D, Discodermolide, and Peloruside A



**A new hydroxide-induced decarboxylative Grob-type fragmentation** for the stereoselective synthesis of methyl-branched trisubstituted olefins, an important motif in many polyketides with interesting biological activity, such as peloruside A, discodermolide,

and epothilone D, is presented. This strategy centers on mesyloxy lactones (see scheme) with three stereogenic centers, one quaternary, which upon treatment with hydroxide fragment extrusion of the leaving group and carbon dioxide to the olefin.





**Underestimated:** The thus far underestimated photo-Fries reaction serves as an efficient tool for the total synthesis of (-)-kendomycin. A powerful ring-closing metathesis is the basis of the

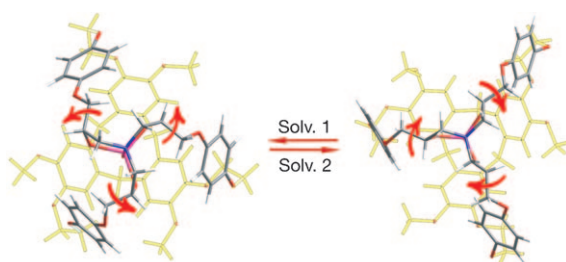
second total synthesis. The installation of the lactol unit was performed by a chemoselective oxidation–hydrolysis sequence, thus avoiding additional protecting groups.

## Total Synthesis

*T. Magauer, H. J. Martin, J. Mulzer\** ..... 507–519

**Ring-Closing Metathesis and Photo-Fries Reaction for the Construction of the Ansamycin Antibiotic Kendomycin: Development of a Protecting Group Free Oxidative Endgame**

VIP



**Solvent-controlled** right or left turn in hemicryptophane–oxidovanadium(V) complexes! The helical chirality of the propeller-like vanatrane moiety gives rise to different diastereomers (see figure). The interconversion between

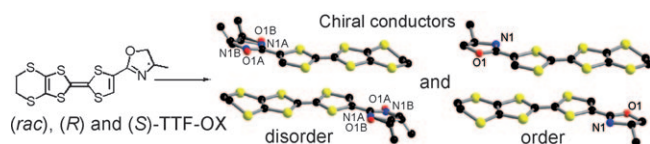
the  $\Lambda$  and  $\Delta$  forms of the propeller is strongly solvent-dependent and the energy barrier is the highest ever reported for atrane derivatives, a consequence of the cage structure.

## Supramolecular Chemistry

*A. Martinez, V. Robert, H. Gornitzka, J.-P. Dutasta\** ..... 520–527

**Controlling Helical Chirality in Atrane Structures: Solvent-Dependent Chirality Sense in Hemicryptophane-Oxidovanadium(V) Complexes**

📖



**Chiral molecular conductors:** Electrocrystallization experiments with the chiral (*R*)-, (*S*)-, and (*rac*)-ethylenedithio-tetrathiafulvalene-methyl-oxazoline (EDT-TTF-OX) donors provide two series of crystalline mixed-valence salts with the  $\text{PF}_6^-$  and  $[\text{Au}(\text{CN})_2]^-$

anions (see figure). The conductivity measurements show metallic behavior in the high-temperature regime with a much lower conductivity when the oxazoline ring is structurally disordered.

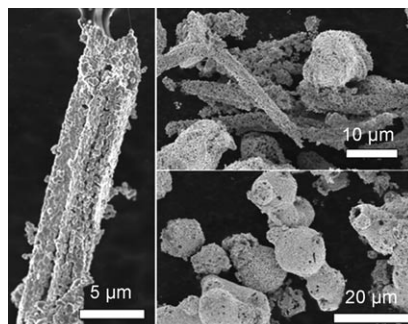
## Conducting Materials

*A. M. Madalan, C. Réthoré, M. Fourmigué, E. Canadell, E. B. Lopes, M. Almeida, P. Auban-Senzier, N. Avarvari\** ..... 528–537

**Order Versus Disorder in Chiral Tetra-thiafulvalene-Oxazoline Radical-Cation Salts: Structural and Theoretical Investigations and Physical Properties**

📖

**Get in shape!** Ag@AgCl samples with hierarchical microstructures including rods, irregular balls, and hollow spheres (see picture) have been fabricated by an ion-exchange process and light-induced chemical reduction reaction. The photocatalytic properties of the samples were evaluated by measuring the decomposition of methyl orange under visible light.



## Heterogeneous Catalysis

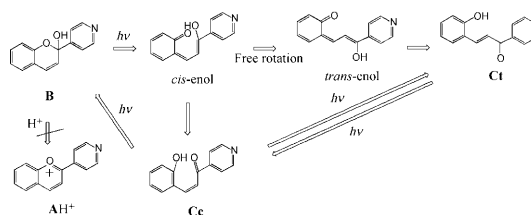
*P. Wang, B. Huang,\* Z. Lou, X. Zhang, X. Qin, Y. Dai, Z. Zheng, X. Wang* ..... 538–544

**Synthesis of Highly Efficient Ag@AgCl Plasmonic Photocatalysts with Various Structures**

## Photochemistry

Y. Leydet, A. J. Parola,\*  
F. Pina\* ..... 545–555

### Hydroxypyridinechromene and Pyridinechalcone: Two Coupled Photochromic Systems



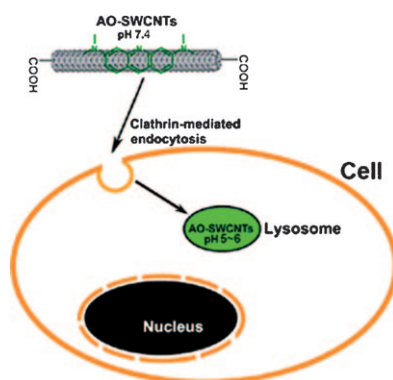
**Significant substitution:** Two coupled photochromic systems that involve hydroxy-4-pyridinechromene and pyridinechalcone are obtained when the

phenyl group in 2-hydroxychalcones is substituted by a 4-pyridine unit (see scheme).

## pH Dependence

X. Zhang, L. Meng, X. Wang,  
Q. Lu\* ..... 556–561

### Preparation and Cellular Uptake of pH-Dependent Fluorescent Single-Wall Carbon Nanotubes

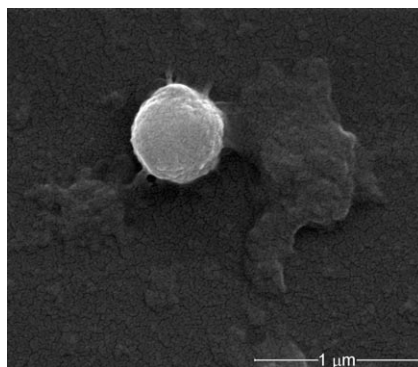


**Orange agent:** The optical absorbance and fluorescence characteristics of acridine orange single-wall carbon nanotube (AO-SWCNT) conjugates display interesting pH-dependent properties. The AO-SWCNTs can enter HeLa cells and are located inside lysosomes by means of clathrin-mediated endocytosis (see picture).

## Core-Shell Structures

N. Skirtenko, T. Tzanov,  
A. Gedanken,\*  
S. Rahimipour\* ..... 562–567

### One-Step Preparation of Multifunctional Chitosan Microspheres by a Simple Sonochemical Method

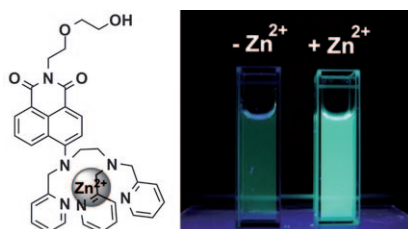


**Modifiable inside and out:** A single-step preparation of chitosan core-shell microspheres (see picture) by a sonochemical method is described. The surface of the microspheres can easily be modified by different electrophiles, while the inside can be loaded with different agents.

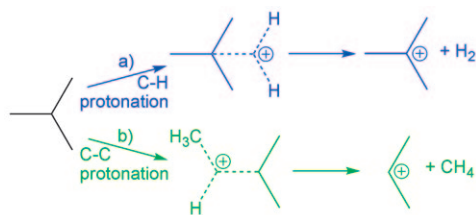
## Fluorescence Spectroscopy

K. Hanaoka, Y. Muramatsu, Y. Urano,  
T. Terai, T. Nagano\* ..... 568–572

### Design and Synthesis of a Highly Sensitive Off-On Fluorescent Chemosensor for Zinc Ions Utilizing Internal Charge Transfer



**Keen sensors!** We present a highly sensitive fluorescent chemosensor based on 4-amino-1,8-naphthalimide, which shows an off-on fluorescence change concomitantly with the appearance of a new absorption band at  $\lambda = 380$  nm in response to zinc ions.



**Super acid for super people:** A super-acid-like activation of alkanes occurs over zeolites. A longstanding controversy about the initial step of hydrocarbon activation on industrial cata-

lysts (a or b, see figure), such as acidic zeolites, has been solved by experiments combining gas chromatography, mass spectroscopy and isotopic labeling of starting materials.

## Alkane Activation

*B. Louis, M. M. Pereira, F. M. Santos, P. M. Esteves, J. Sommer\* . . . . 573–576*

## Alkane Activation over Acidic Zeolites: The First Step



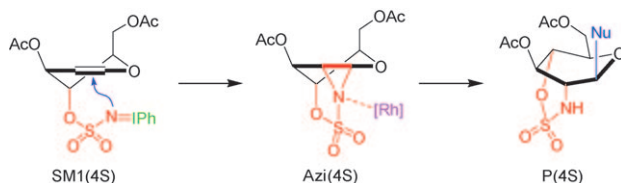
**What an effect:** A new subclass of  $\beta$ -aminoxy peptides, that is, peptides of acyclic  $\beta^{2,3}$ -aminoxy acids (see picture), has been synthesized and the effect of the backbone stereochemistry on their conformations provides a useful insight into the design and construction of new foldamers with predicable structures.



## Peptides

*Y.-H. Zhang, K. Song, N.-Y. Zhu, D. Yang\* . . . . . 577–587*

## The Effect of Backbone Stereochemistry on the Folding of Acyclic $\beta^{2,3}$ -Aminoxy Peptides



**The journey is the reward:** DFT calculations and experimental observations were combined to elucidate the mechanistic pathway of rhodium-catalyzed aziridination and ring opening on a

glycal scaffold (see scheme). The installation of a sulfamate moiety at different positions of the glycal scaffold could present a new concept for synthesizing  $\alpha$ - and  $\beta$ -aminoglycosides.

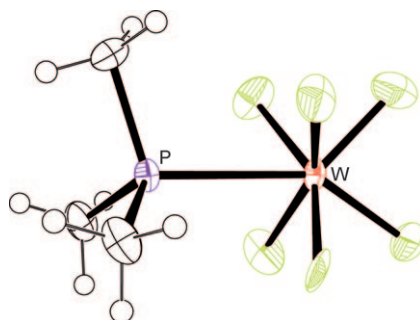
## DFT Calculations

*R. Lorpithaya, Z.-Z. Xie, K. B. Sophy, J.-L. Kuo,\* X.-W. Liu\* . . . . . 588–594*

## Mechanistic Insights into the Substrate-Controlled Stereochemistry of Glycals in One-Pot Rhodium-Catalyzed Aziridination and Aziridine Ring Opening



**Cat got your tungsten?** In the present work the transition between complex formation and redox chemistry of tungsten(VI) fluorides with phosphanes is studied (see figure). The complexes studied are characterised by using H, F, and P NMR spectroscopy; EPR and IR spectroscopy; and single-crystal X-ray analysis.



## Tungsten Complexes

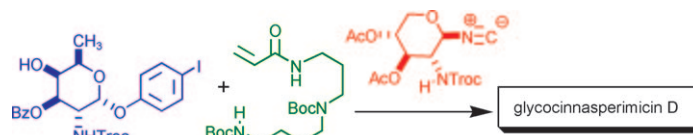
*S. El-Kurdi, A.-A. Al-Terkawi, B. M. Schmidt, A. Dimitrov, K. Seppelt\* . . . . . 595–599*

## Tungsten(VI) and Tungsten(V) Fluoride Complexes

## Antibiotics

T. Nishiyama, Y. Kusumoto,  
K. Okumura, K. Hara, S. Kusaba,  
K. Hirata, Y. Kamiya, M. Isobe,  
K. Nakano, H. Kotsuki,  
Y. Ichikawa\* ..... 600–610

### Synthesis of Glycocinnasperimicin D



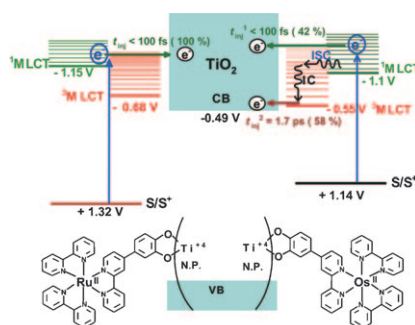
**Nitrogen-rich antibiotic:** The synthetic venture of glycocinnasperimicin D, an amino sugar antibiotic decorated with a variety of nitrogen-containing functional groups, has been completed by a three-component coupling strategy

(see scheme). The convergent tactic is realized by the Heck–Mizoroki reaction and construction of the urea glycoside by the reaction of glycosyl isocyanate with an amino sugar.

## Electron Transfer

S. Verma, P. Kar, A. Das,\* D. K. Palit,  
H. N. Ghosh\* ..... 611–619

### The Effect of Heavy Atoms on Photo-induced Electron Injection from Nonthermalized and Thermalized Donor States of $M^{II}$ –Polypyridyl ( $M=Ru/Os$ ) Complexes to Nanoparticulate $TiO_2$ Surfaces: An Ultrafast Time-Resolved Absorption Study

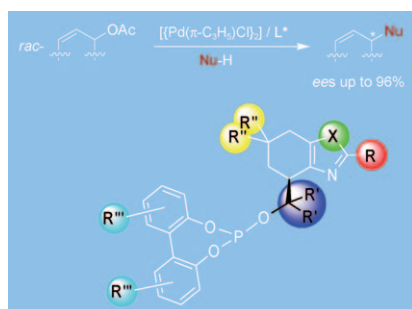


**Ultrafast studies:** Two polypyridyl complexes— $[M(bpy)_2L]^{2+}$ , in which  $M=Ru^{II}$  or  $Os^{II}$ ,  $bpy=2,2'$ -bipyridyl, and  $L=4-(2,2'$ -bipyridinyl-4-yl)benzene-1,2-diol—have been synthesized and their interfacial electron-transfer process on a  $TiO_2$  nanoparticle surface has been studied with femtosecond transient-absorption spectroscopy (see image).

## Ligand Design

J. Mazuela, A. Paptchikhine, P. Tolstoy,  
O. Pàmies, M. Diéguez,\*  
P. G. Andersson\* ..... 620–638

### A New Class of Modular P,N-Ligand Library for Asymmetric Pd-Catalyzed Allylic Substitution Reactions: A Study of the Key Pd– $\pi$ -Allyl Intermediates

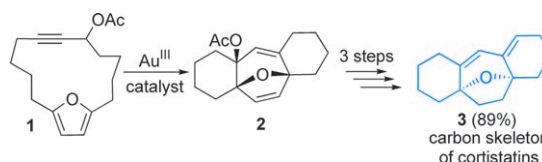


**Substrate substitutions:** We describe the synthesis and application of a library of phosphite–oxazole/thiazole ligands in the Pd-catalyzed allylic substitution reactions of several substrate types (see scheme). High regio- and enantioselectivities and good activities have been achieved.

## Transannular Cycloaddition

B. W. Gung,\* D. T. Craft, L. N. Bailey,  
K. Kirschbaum ..... 639–644

### Gold-Catalyzed Transannular [4 + 3] Cycloaddition Reactions

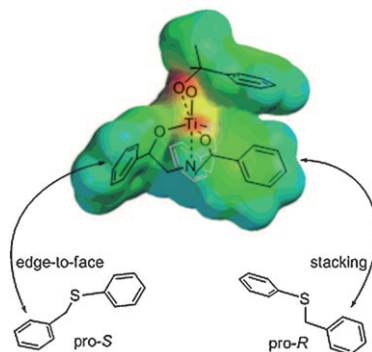


**The synthesis of a tetracyclic ring system under Au catalysis:** Macrocyclic propargyl esters (**1**) undergo a tandem 3,3-rearrangement/transannular [4 + 3] cycloaddition reaction in the presence of a  $Au^{III}$  catalyst to give a multiple

fused-ring structure (**2**). The tetracyclic carbon core structure (**3**) of the potent antiangiogenesis natural product cortistatin A, which features a conjugated diene functionality, was easily obtained from **2**.



**$\pi$ - $\pi$  versus  $\pi$ - $\pi$ :** Stereoselectivity of an oxygen-transfer reaction catalysed by  $\text{Ti}^{\text{IV}}$  trialkanolamines (see scheme) is determined by the subtle interplay of edge-to-face and face-to-face aromatic interactions.



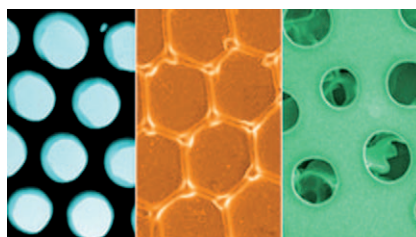
## Catalytic Oxidation

G. Santoni, M. Mba, M. Bonchio,  
W. A. Nugent, C. Zonta,\*  
G. Licini\* ..... 645–654

**Stereoselective Control by Face-to-Face Versus Edge-to-Face Aromatic Interactions: The Case of  $\text{C}_3$ - $\text{Ti}^{\text{IV}}$  Amino Trialkolate Sulfoxidation Catalysts**



**Golden honeycombs:** Ligand-stabilized gold nanoparticles are used as building blocks to fabricate macroporous films with ordered honeycomb structures at an air/water interface. The films' fabrication is based on solvent evaporation and templated by water droplets; morphological changes in the films are dependent on the concentration of gold nanoparticles. Both two- and three-dimensional pore arrays are observed (see picture).



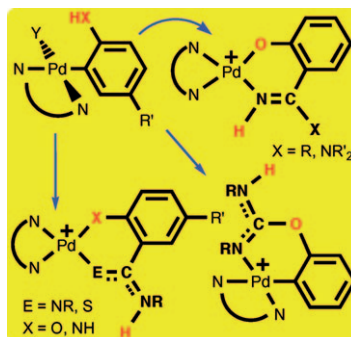
## Porous Films

H. Ma, J. Hao\* ..... 655–660

**Evaporation-Induced Ordered Honeycomb Structures of Gold Nanoparticles at the Air/Water Interface**



**Unusual insertion:** A series of *ortho*-substituted aryl-palladium(II) complexes have been reacted with unsaturated N-donor ligands giving insertion and/or addition products (see scheme).

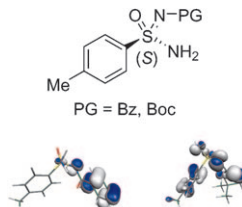


## Insertion Reactions

J. Vicente,\* J.-A. Abad,  
M.-J. López-Sáez, P. G. Jones,  
D. Bautista ..... 661–676

**Reactivity of *ortho*-Substituted Aryl-Palladium Complexes towards Carbodiimides, Isothiocyanates, Nitriles, and Cyanamides**

**Sulfonimidamides in three dimensions:** The absolute configurations of enantiopure *N*-protected sulfonimidamides, which have been accessed through straightforward syntheses, were assigned by X-ray structure determination and comparison of calculated and measured CD spectra (see scheme).




## Organic Chemistry

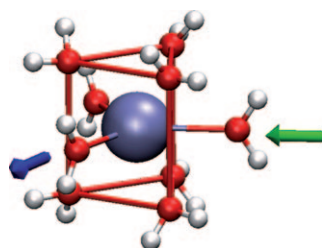
C. Worch, I. Atodiresi, G. Raabe,  
C. Bolm\* ..... 677–683

**Synthesis of Enantiopure Sulfonimidamides and Elucidation of Their Absolute Configuration by Comparison of Measured and Calculated CD Spectra and X-Ray Crystal Structure Determination**

## Structure Determination

P. D'Angelo,\* A. Zitolo, V. Migliorati,  
I. Persson ..... 684–692


 **Analysis of the Detailed Configuration of Hydrated Lanthanoid(III) Ions in Aqueous Solution and Crystalline Salts by Using K- and L<sub>3</sub>-Edge XANES Spectroscopy**

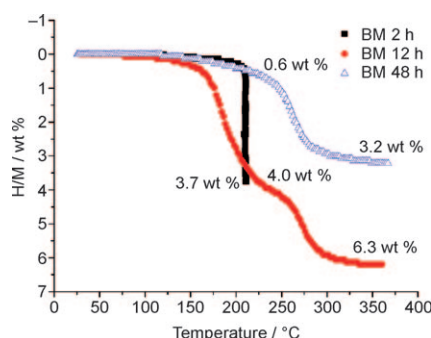


**A smooth transition:** X-ray absorption near-edge structure (XANES) spectroscopy has been found to be the ideal experimental technique to shed light on the structure of the hydration complexes of the Ln<sup>III</sup> ions in aqueous solution. The analysis of the XANES spectra has provided definitive experimental proof of the retention of the tricapped trigonal prism geometry (see figure) of the Ln<sup>III</sup> hydrated ions along the series.

## Hydrogen Storage

C. Liang, Y. Liu,\* K. Luo, B. Li,  
M. Gao, H. Pan,\* Q. Wang ... 693–702

 **Reaction Pathways Determined by Mechanical Milling Process for Dehydrogenation/Hydrogenation of the LiNH<sub>2</sub>/MgH<sub>2</sub> System**




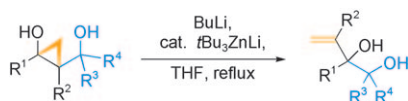
### Keeping our eye on the ball (milling)!

The reaction pathways for hydrogen desorption/absorption of the LiNH<sub>2</sub>/MgH<sub>2</sub> (1:1) system were found to depend strongly on the ball-milling duration (BM; see figure). This is due to the presence of two competing reactions in different stages including the ball milling and the heating process.

## Rearrangement

K. Nomura, S. Matsubara\* ... 703–708


 **A New Zincate-Mediated Rearrangement Reaction of 2-(1-Hydroxyalkyl)-1-alkylcyclopropanol**

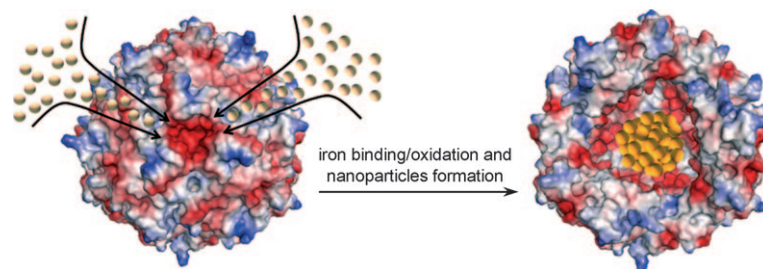


**Catalytic zincate:** A novel rearrangement of 2-(1-hydroxyalkyl)-1-alkylcyclopropanol, which proceeds in the presence of a catalytic amount of organozinc ate complex to give *vic*-diols (see scheme), has been found. The rearrangement can be applied to various types of 2-(1-hydroxyalkyl)-1-alkylcyclopropanol, which can be easily prepared from the corresponding  $\alpha,\beta$ -epoxyketones and bis(iodozincio)methane.

## Magnetic Nanoparticles

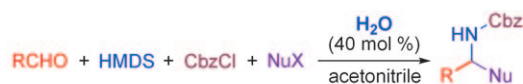
P. Ceci, E. Chiancone, O. Kasyutich,  
G. Bellapadrona, L. Castelli,  
M. Fittipaldi, D. Gatteschi,  
C. Innocenti, C. Sangregorio\* 709–717

 **Synthesis of Iron Oxide Nanoparticles in *Listeria innocua* Dps (DNA-Binding Protein from Starved Cells): A Study with the Wild-Type Protein and a Catalytic Centre Mutant**



**Grown in a cavity:** The magnetic properties of 3 nm iron oxide nanoparticles grown in the cavity of the DNA-binding protein from starved cells of the bacterium *Listeria innocua*, and in its

triple-mutant, lacking the catalytic ferroxidase centre, have been investigated by TEM and static and dynamic magnetic and electron magnetic resonance measurements (see figure).



Nu = H, allyl, CH(COR)CO<sub>2</sub>Et, CH(COR)<sub>2</sub>, CHR(COR')  
X = SiR<sub>3</sub>, H

**Byproduct catalysis:** Four-component reactions of aldehydes with hexamethyldisilazane (HMDS), chloroformates, and nucleophiles have been developed by using a catalytic amount of water to produce various protected

primary amines, β-amino esters, and β-amino ketones (see scheme; CbzCl: benzyl chloroformate). No catalyst is needed for the reactions with aldehydes bearing hydroxy groups.

## Multicomponent Reactions

B.-L. Yang, Z.-T. Weng, S.-J. Yang, S.-K. Tian\* ..... 718–723

**Byproduct-Catalyzed Four-Component Reactions of Aldehydes with Hexamethyldisilazane, Chloroformates, and Nucleophiles in Acetonitrile Leading to Protected Primary Amines, β-Amino Esters, and β-Amino Ketones**

\* Author to whom correspondence should be addressed

Supporting information on the WWW (see article for access details).

**VIP** Full Papers labeled with this symbol have been judged by two referees as being “very important papers”.

A video clip is available as Supporting Information on the WWW (see article for access details).

## SERVICE

Spotlights ..... 398      Author Index ..... 726      Keyword Index ..... 727      Preview ..... 729

Issue 1/2010 was published online on December 22, 2009



**Fast, Individual, Popular...**  
**REPRINTS**  
**Available to order anytime!**  
Contact Carmen Leitner (e-mail: chem-reprints@wiley.com)